TMEM16F is required for phosphatidylserine exposure and microparticle release in activated mouse platelets

Toshihiro Fujii[a,b], Asuka Sakata[c], Satoshi Nishimura[c,d], Koji Eto[e], and Shigekazu Nagata[a,b,1]

[a]Laboratory of Biochemistry & Immunology, Immunology Frontier Research Center, Osaka University, Osaka 565-0871, Japan; [b]Core Research for Evolutional Science and Technology, Japan Science and Technology Agency, Saitama 332-0012, Japan; [c]Center for Molecular Medicine, Jichi Medical University, Tochigi 329-0498, Japan; [d]Department of Cardiovascular Medicine, The University of Tokyo, Tokyo 113-0033, Japan; and [e]Department of Clinical Application, Center for iPS Cell Research and Application, Kyoto University, Kyoto 606-8507, Japan

Contributed by Shigekazu Nagata, August 20, 2015 (sent for review July 13, 2015; reviewed by Yuzuru Kanakura, Tatsutoshi Nakahata, and Kiyoshi Takatsu)

Phosphatidylserine (PtdSer) exposure on the surface of activated platelets requires the action of a phospholipid scramblase(s), and serves as a scaffold for the assembly of the tenase and prothrombinase complexes involved in blood coagulation. Here, we found that the activation of mouse platelets with thrombin/collagen or Ca^{2+} ionophore at 20 °C induces PtdSer exposure without compromising plasma membrane integrity. Among five transmembrane protein 16 (TMEM16) members that support Ca^{2+}-dependent phospholipid scrambling, TMEM16F was the only one that showed high expression in mouse platelets. Platelets from platelet-specific *TMEM16F*-deficient mice exhibited defects in activation-induced PtdSer exposure and microparticle shedding, although α-granule and dense granule release remained intact. The rate of tissue factor-induced thrombin generation by *TMEM16F*-deficient platelets was severely reduced, whereas thrombin-induced clot retraction was unaffected. The imaging of laser-induced thrombus formation in whole animals showed that PtdSer exposure on aggregated platelets was TMEM16F-dependent in vivo. The phenotypes of the platelet-specific *TMEM16F*-null mice resemble those of patients with Scott syndrome, a mild bleeding disorder, indicating that these mice may provide a useful model for human Scott syndrome.

platelets | phosphatidylserine | microvesicles | scramblase | calcium

Phospholipids are asymmetrically distributed between the inner and outer leaflets of plasma membranes as a result of the activity of flippase(s), which specifically translocates phosphatidylserine (PtdSer) and phosphatidylethanolamine from the outer to the inner leaflet of plasma membranes (1). PtdSer is preferentially exposed on the cell surface during certain physiological processes. During apoptosis, cell-surface PtdSer functions as an "eat me" signal to induce engulfment by phagocytic cells, and, during platelet activation, it serves as a scaffold for the activation of clotting factors. Exposed PtdSer is also implicated in pathological processes and may promote the retention of Ca^{2+} oxalate in kidneys, leading to kidney stone formation (2).

PtdSer exposure is accomplished by the inactivation of flippase(s), along with the activation of scramblases (3). We recently identified two protein families (TMEM16 and Xkr) that support phospholipid scrambling (4–6). The TMEM16 family consists of 10 members with 10 transmembrane regions, and TMEM16C, 16D, 16F, 16G, and 16J support the Ca^{2+}-dependent scrambling of phospholipids. Scott syndrome is a mild bleeding disorder caused by a defect in platelet procoagulant activity (7, 8). Platelets, red blood cells, and EBV-transformed B cells from patients with Scott syndrome exhibit defective PtdSer exposure following platelet activation or treatment with Ca^{2+} ionophore (9–11). We and others reported that patients with Scott syndrome carry null mutations in the TMEM16F gene (6, 12).

The fetal thymocyte cell lines established from *TMEM16F*$^{-/-}$ mouse embryos exhibit defective PtdSer exposure upon treatment with Ca^{2+} ionophore (5), reminiscent of the EBV-transformed B-cell lines from patients with Scott syndrome. In contrast, Yang et al. (13) reported that *TMEM16F*-deficient mouse platelets exhibit only a mild defect in Ca^{2+}ionophore–induced PtdSer exposure and tissue factor-induced thrombin generation. Furthermore, in contrast to a human patient with Scott syndrome (14) and dogs with a similar hereditary syndrome (15), neither of which exhibits apparent bleeding-time defects, *TMEM16F*$^{-/-}$ mice exhibit a prolonged bleeding time—twice that of WT mice (13).

To address the apparent discrepancies between *TMEM16F*$^{-/-}$ mouse phenotypes and the clinical presentation of patients with Scott syndrome, and to examine the role of platelet-expressed TMEM16F in blood clotting, we generated a platelet-specific *TMEM16F* deletion in mice. Our in vitro and in vivo analyses of thrombus formation induced by *TMEM16F*-null platelets suggested a role for TMEM16F in activation-induced PtdSer exposure, and supported the model in which Ca^{2+}-induced PtdSer exposure is involved in the generation of thrombin and fibrin, but not clot retraction (16, 17). Mice with the platelet-specific deletion of TMEM16F exhibited a phenotype similar to that of human patients with Scott syndrome, and may provide a useful model for this human disease.

Results

PtdSer Exposure on Activated Mouse Platelets. The activation of platelets with thrombin, collagen, or Ca^{2+} ionophore induces PtdSer exposure (18). However, platelet activation often causes rupture (19), which complicates the determination of whether the PtdSer exposure is caused by phospholipid scrambling at the plasma membrane or the rupture of plasma membranes. Apoptotic

Significance

In activated platelets, a scramblase(s) scrambles phospholipids at plasma membranes and exposes phosphatidylserine (PtdSer) to the surface. PtdSer on activated platelets serves as a scaffold for the tenase and prothrombinase complexes for blood coagulation. Among five transmembrane protein 16 (TMEM16) members that support Ca^{2+}-dependent phospholipid scrambling, TMEM16F is highly expressed in mouse platelets, and is indispensable for activation-induced PtdSer exposure and microparticle shedding. Thus, the rate of platelet-induced thrombin generation is severely reduced by the *TMEM16F* deficiency. The role of TMEM16F in PtdSer exposure on aggregated platelets is also shown in vivo with laser-induced thrombus formation. The phenotypes of *TMEM16F*-null mice resemble those of patients with Scott syndrome, a mild bleeding disorder, indicating that these mice provide a good model for this disease.

Author contributions: T.F., S. Nishimura, K.E., and S. Nagata designed research; T.F., A.S., and S. Nishimura performed research; T.F., K.E., and S. Nagata analyzed data; and T.F., S. Nishimura, K.E., and S. Nagata wrote the paper.

Reviewers: Y.K., Osaka University Graduate School of Medicine; T.N., Center for iPS Cell Research and Application, Kyoto University; and K.T., University of Toyama.

The authors declare no conflict of interest.

[1]To whom correspondence should be addressed. Email: snagata@ifrec.osaka-u.ac.jp.

This article contains supporting information online at www.pnas.org/lookup/suppl/doi:10.1073/pnas.1516594112/-/DCSupplemental.

stimuli cause apoptotic cell death and PtdSer exposure, but can also cause necrosis, particularly when the stimuli are strong and cells are exposed to them for long periods (20). To distinguish apoptosis-induced PtdSer exposure from that caused by necrosis, cells are usually stained with membrane-impermeable DNA-staining dyes together with PtdSer-staining reagents (21). However, such dyes cannot be used for staining platelets because they lack nuclei. Because phalloidin, which is also a membrane-impermeable reagent, binds to F-actin in the cytoplasm (22), we reasoned that phalloidin staining could be useful in identifying and excluding necrotic cells from the analysis of PtdSer-exposing platelets.

W3 cells, which are mouse T-cell leukemia WR19L cells expressing Fas (23), were treated with FasL (24) and stained with SYTOX Blue or phalloidin, together with Annexin V. Resting W3 cells were negative for Annexin V and SYTOX Blue staining (Fig. S1). At 2 h after the addition of FasL, 85% of the cells were Annexin V-positive but SYTOX Blue-negative, indicating that most of the cells underwent apoptosis. As the incubation continued, SYTOX Blue-positive cells were detected, and, at 4 h after the FasL addition, more than 90% of the cells were positive for Annexin V and SYTOX Blue, indicating that they were undergoing necrosis. Staining with Annexin V and phalloidin resulted in similar cell profiles; W3 cells treated with FasL for 2 h were Annexin V-positive and phalloidin-negative, whereas the 4-h treated cells were positive for Annexin V and phalloidin, indicating that phalloidin staining can be used to exclude plasma membrane-compromised cells.

Human and mouse platelets were stimulated for 5 min at 37 °C with 0.5 U/mL thrombin and 10 μg/mL collagen, or with 1.0 μM A23187 in the presence of 1.0 mM $CaCl_2$, and stained with Annexin V and phalloidin. As shown in Fig. 1, the stimulated human platelets exposed PtdSer and were Annexin V-positive, but they remained phalloidin-negative. In contrast, the stimulated mouse platelets were Annexin V- and phalloidin-positive, indicating that they had undergone necrosis. However, when the mouse platelets were treated with thrombin and collagen, or A23187 at 20 °C instead of 37 °C, Annexin V- but not phalloidin-positive cells were detected at 5 min after treatment. When the 20 °C-activated cells were permeabilized with 0.3% saponin, phalloidin-positive cells were detected, consistent with the premise that membrane rupture of the activated platelets was prevented by lowering the incubation temperature. These results suggested that the activated mouse platelets exposing PtdSer were fragile and susceptible to membrane rupture at 37 °C. Therefore, the in vitro effect of TMEM16F on PtdSer exposure in mouse platelets was examined at 20 °C throughout the rest of the study.

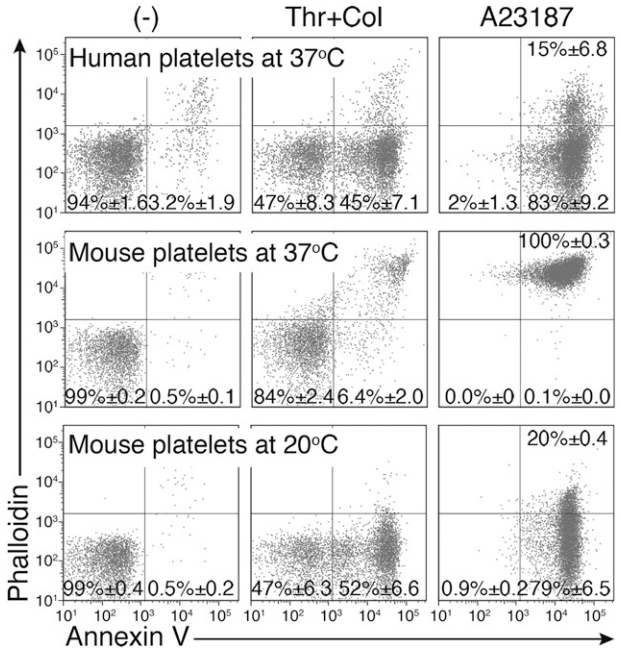

Fig. 1. PtdSer exposure on activated mouse platelets. Human and murine platelets were treated for 5 min at 20 °C or 37 °C with 0.5 U/mL thrombin plus 10 μg/mL collagen or 1 μM A23187 in Tyrode-H buffer containing 1 mM $CaCl_2$. The cells were stained with Cy5-Annexin V and Alexa Fluor 488-phalloidin and analyzed by flow cytometry. The experiments were performed three times, and the average values are shown with SD.

PtdSer Exposure in Activated Mouse Platelets Requires TMEM16F. Among 10 TMEM16 members, TMEM16C, 16D, 16F, 16G, and 16J support phospholipid scramblase activity (5). Human platelets expressed a high level of TMEM16F, but not other members (Fig. S2). Accordingly, real-time RT-PCR analysis showed that mouse platelets expressed a high level of TMEM16F and low levels of TMEM16B, 16H, and 16K mRNAs (Fig. 2*A*), suggesting that TMEM16F could play a role in phospholipid scrambling in mouse platelets. Mice carrying *TMEM16F*-floxed alleles (*TMEM16F*$^{fl/fl}$) (5) were crossed with Platelet factor 4 (Pf4)-CRE mice, which express CRE recombinase under the control of the megakaryocyte/platelet-specific Pf4 promoter (25). A Western blot analysis with anti-TMEM16F antibody showed the presence of a broad band of ∼120 kDa in platelets from *TMEM16F*$^{fl/fl}$ mice (Fig. 2*B*), which was absent in the platelets from *TMEM16F*$^{fl/fl}$;*Pf4-CRE* mice. Mouse TMEM16F contains three N-glycosylation sites (6), which could explain the heterogeneity of the TMEM16F protein on Western blots.

Platelets from *TMEM16F*$^{fl/fl}$ and *TMEM16F*$^{fl/fl}$;*Pf4-CRE* mice were then stimulated for 5 min at 20 °C with thrombin and collagen in the presence of 1.0 mM $CaCl_2$. As shown in Fig. 2*C*, PtdSer exposure was detected in ∼20% of the stimulated TMEM16F-expressing platelets, whereas the stimulated *TMEM16F*-deficient platelets showed minimal PtdSer exposure. In contrast, these stimuli increased the intracellular Ca^{2+} concentrations of the control and *TMEM16F*-deficient platelets (Fig. S3*A*), indicating that TMEM16F plays an essential role in PtdSer exposure in activated mouse platelets. Activated platelets also release various granules, such as α-granules containing P-selectin and dense granules containing ATP (26, 27). When platelets from *TMEM16F*$^{fl/fl}$ and *TMEM16F*$^{fl/fl}$;*Pf4-CRE* mice were activated with thrombin and collagen, more than 90% of the platelets with both genotypes expressed P-selectin (Fig. S3*B*). In addition, both *TMEM16F*-expressing and -deficient platelets released similar amounts of ATP in response to thrombin/collagen or A23187 (Fig. S3*C*). These results indicated that TMEM16F was not involved in the release of α- and dense granules.

Involvement of TMEM16F in the Release of Microparticles. Activated platelets also release microparticles (28), and this process depends on calpain and/or phospholipid scramblase(s) (9, 10). To examine the contribution of TMEM16F to this process, platelets from *TMEM16F*$^{fl/fl}$ or *TMEM16F*$^{fl/fl}$;*Pf4-CRE* mice were treated with thrombin and collagen in the presence of 1.0 mM $CaCl_2$ and analyzed by flow cytometry. As shown in Fig. 3*A*, the activation of *TMEM16F*-expressing platelets for 5 min resulted in generation of a population of particles characterized by reduced forward scatter (FSC). In contrast, stimulated *TMEM16F*-deficient platelets showed little change in FSC, supporting the idea that TMEM16F-mediated phospholipid scrambling plays an important role in microparticle shedding from activated platelets.

Platelets undergo dramatic changes in morphology upon binding to immobilized adhesive proteins (29). As shown in Fig. 3*B*, when purified *TMEM16F*-expressing or -deficient platelets were allowed to adhere to fibrinogen-coated plates and observed

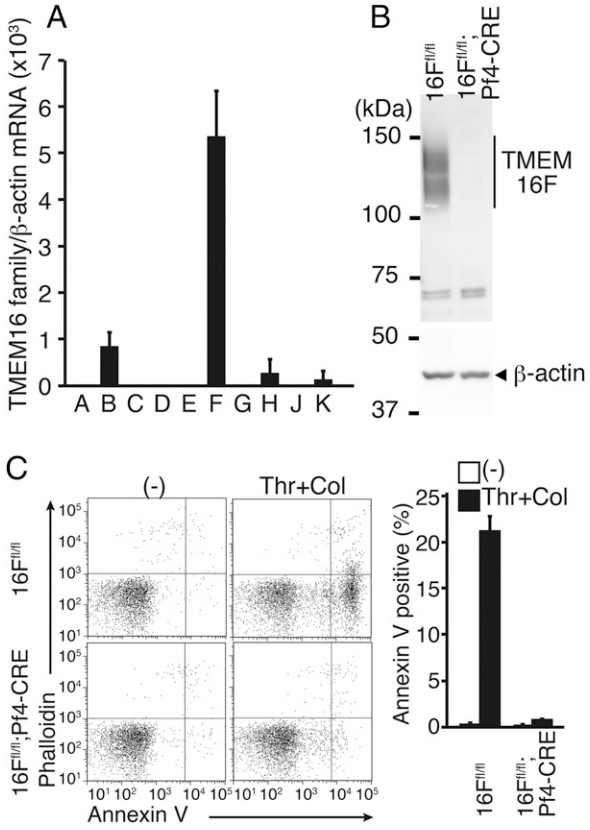

Fig. 2. Requirement of TMEM16F for PtdSer exposure on activated mouse platelets. (*A*) TMEM16 family expression in mouse platelets. RNA from mouse platelets was subjected to real-time RT-PCR for the 10 TMEM16 family members. Each mRNA level is expressed relative to β-actin mRNA. The experiments were performed three times, and the average values are shown with SD (bars). (*B*) TMEM16F Western blotting of mouse platelets. Cell lysates (5 μg protein) from platelets of *TMEM16F*$^{fl/fl}$ and *TMEM16F*$^{fl/fl}$*;Pf4-CRE* mice were analyzed by Western blotting with anti-TMEM16F. The TMEM16F band is indicated. (*C*) Platelets from *TMEM16F*$^{fl/fl}$ and *TMEM16F*$^{fl/fl}$*;Pf4-CRE* mice were treated at 20 °C for 5 min with 0.5 U/mL thrombin plus 10 μg/mL collagen (Thr + Col) in Tyrode-H buffer with 1 mM $CaCl_2$. The activated platelets were stained with phycoerythrin/cyanin 7 (PE/Cy7)–anti-CD41 mAb, Cy5-Annexin V, and Alexa Fluor 488-phalloidin (*C*) and analyzed by flow cytometry. FACS profiles for phalloidin and Annexin V staining in the CD41-positive population are shown. The experiments were performed three times, and the percentages of Annexin V-positive and phalloidin-negative populations are plotted (*Right*) with SD (bars).

by scanning EM, within 2 h they exhibited a marked central mounding. There was no difference in the morphologies of resting *TMEM16F*-expressing and -deficient platelets. When the platelets on fibrinogen-coated dishes were stimulated with 1.0 μM A23187 in the presence of 1.0 mM $CaCl_2$, both types of platelets generated many rod-like extensions arranged in a concentric pattern within 1 min (Fig. 3*B*). However, 3–5 min later, whereas most of the rod-like extensions and central moundings of the *TMEM16F*-expressing platelets had been replaced by flattened structures, the rod-like extensions continued to develop in the *TMEM16F*-deficient platelets, and the central moundings remained in most of them. These results indicated that the microparticle shedding and breakdown of the rod-like membrane extensions in platelets were similarly regulated by TMEM16F.

TMEM16F-Dependent Thrombin Generation. PtdSer exposed on the platelets serves as the membrane scaffold for tenase (Factors VIII and IX) and prothrombinase (Factors V and X), resulting in the generation of thrombin for blood clotting (17). To investigate the possible involvement of TMEM16F in thrombin generation, the tissue factor-induced thrombin generation was assayed at 20 °C with platelet-free plasma (PFP) and washed *TMEM16F*-expressing or -deficient platelets. As shown in Fig. 4*A*, the thrombin activity generated with *TMEM16F*-expressing platelets began to increase at 8 min and peaked ∼15–18 min after the addition of tissue factor. *TMEM16F*-deficient platelets also supported the thrombin generation to some extent. This is probably because of the necrosis that occurred in the activated platelets after the longer incubation. Notably, the initial rate of thrombin production mediated by the *TMEM16F*-deficient platelets was 5–10 fold lower than that associated with the *TMEM16F*-expressing platelets. Furthermore, addition of the D89E mutant of MFG-E8, which masks PtdSer (21), to the thrombin generation assay dose-dependently inhibited thrombin generation by the *TMEM16F*-expressing and -deficient platelets (Fig. 4*B*), confirming that PtdSer exposed on platelets played an essential role in activating tenase and prothrombinase. The prothrombin and

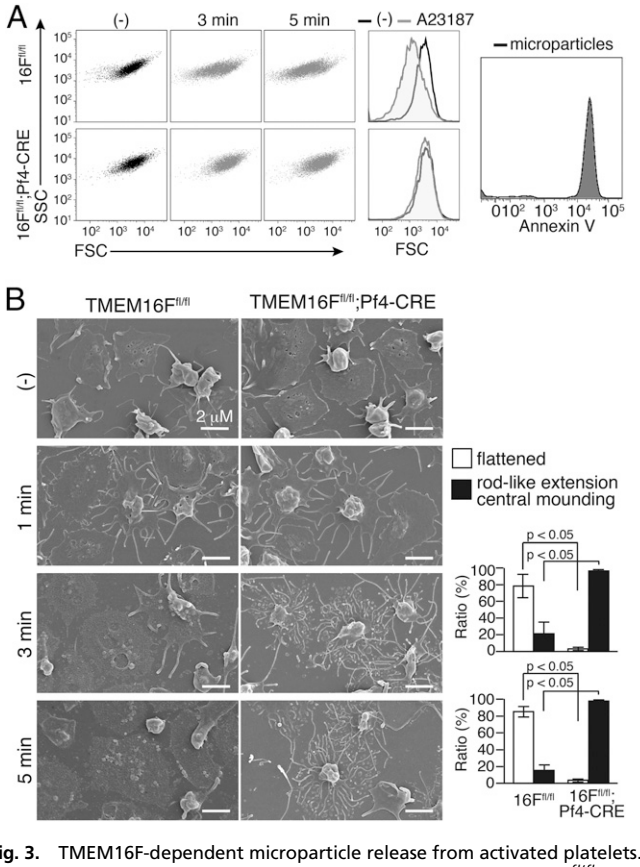

Fig. 3. TMEM16F-dependent microparticle release from activated platelets. (*A*) TMEM16F-dependent microparticle formation. *TMEM16F*$^{fl/fl}$ and *TMEM16F*$^{fl/fl}$*;Pf4-CRE* platelets (4×10^5) were left untreated or treated with 1 μM A23187 in 0.2 mL of Tyrode-H buffer with 1 mM $CaCl_2$ at 20 °C for 3 or 5 min and stained with CD41-PE/Cy7. The FSC/side scatter (SSC) profiles of CD41-positive populations are shown. (*Center*) Merged FSC profiles in unstimulated or 5-min stimulated platelets. (*Right*) Microparticles were collected by centrifugation from the stimulated WT platelets and stained with Cy5-Annexin V. (*B*) Scanning EM images of activated platelets. *TMEM16F*$^{fl/fl}$ and *TMEM16F*$^{fl/fl}$*;Pf4-CRE* platelets (3×10^5) were left unstimulated or stimulated as in *A* with 1 μM A23187 for 1, 3, or 5 min in the presence of 1 mM $CaCl_2$. The adherent platelets were observed by scanning EM. (Scale bar: 2 μm.) The 3-min or 5-min activated platelets (approximately 300 platelets in three fields for each) were classified into flattened or rod-like extension and central mounting categories, and their percentages are plotted (*Right*). The Student *t* test was used for statistical analysis, and *P* values are shown.

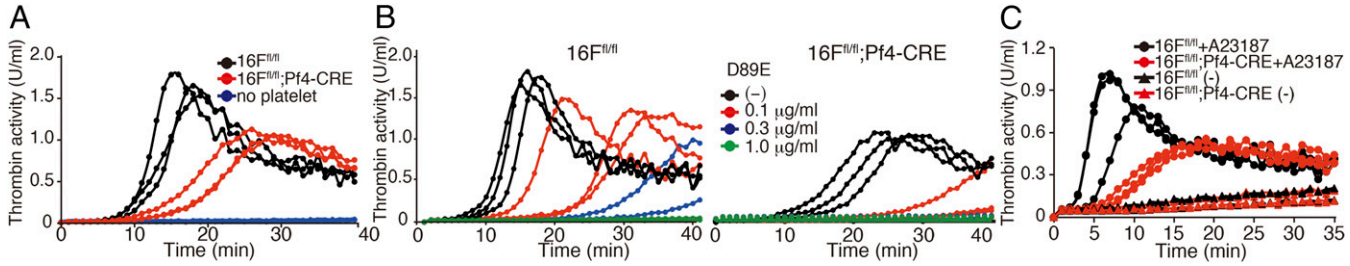

Fig. 4. Contribution of TMEM16F to PtdSer-mediated thrombin formation by platelets and microparticles. (*A* and *B*) Thrombin generation assay with TMEM16F-expressing or -deficient platelets. Washed platelets (1.2×10^7, three independent preparations each) from *TMEM16F*$^{fl/fl}$ or *TMEM16F*$^{fl/fl}$;*Pf4-CRE* mice were mixed with 6 μL of PFP in 120 μL Tyrode-H buffer containing 8 mM $CaCl_2$ in the absence (*A*) or presence of 0.1, 0.3, or 1.0 μg/mL D89E (*B*) and incubated at 20 °C with 8.3 pM human tissue factor. Thrombin activity was assayed with Z-GGR-AMC. (*C*) Thrombin generation by microparticles. Platelets (1.2×10^7) from *TMEM16F*$^{fl/fl}$ or *TMEM16F*$^{fl/fl}$;*Pf4-CRE* platelets (three independent preparations each) were stimulated at 20 °C for 5 min with 1 μM A23187 or left unstimulated in Tyrode-H buffer containing 1 mM $CaCl_2$. The microparticles were collected and used for thrombin generation.

activated partial thromboplastin times were comparable when PFP from the *TMEM16F*-expressing or -deficient mice was used (Table S1), confirming that the TMEM16F required for thrombin generation was intrinsic to platelets.

Microparticles released from activated platelets can also activate the tenase and prothrombinase complexes to promote coagulation (30). Microparticles collected from A23187-treated *TMEM16F*-expressing platelets constitutively exposed PtdSer on their surface (Fig. 3*A*) and generated thrombin in the presence of PFP with no or minimal delay (Fig. 4*C*). Consistent with the finding that few microparticles were released from the *TMEM16F*-deficient platelets (Fig. 3*A*), the ability of microparticles collected from A23187-treated *TMEM16F*-deficient platelets to support thrombin generation was low. Another role of platelets in thrombus formation involves their aggregation and subsequent contribution to fibrin clot retraction. When *TMEM16F*-expressing and -deficient platelets were stimulated with thrombin, the clot retraction occurred in less than 90 min, and there was no clear difference in their rates or levels (Fig. S4*A*). Accordingly, the tail bleeding times were similar in the *TMEM16F*-expressing and -deficient mice (Fig. S4*B*).

TMEM16F-Dependent Thrombus Formation in Vivo. The numbers of platelets, erythrocytes, and white blood cells, as well as the hematological parameters, were comparable between *TMEM16F*-expressing and -deficient mice (Table S1). The contribution of TMEM16F to in vivo thrombus formation and PtdSer exposure in vivo was examined by using intravital visualization technique (31). Platelet aggregations in testicular veins were induced by reactive oxygen species (ROS) produced by photochemical reactions with laser irradiations, and the developed thrombus area within vessel lumens was quantified. In *TMEM16F*-deficient mice, near-normal platelet aggregation responses were observed in the early phase (40 s after laser irradiation; Fig. 5 *A* and *B* and Movies S1*A* and S1*B* and S2*A* and S2*B*), and thrombus development in *TMEM16F*-deficient mice was similar to that in control mice.

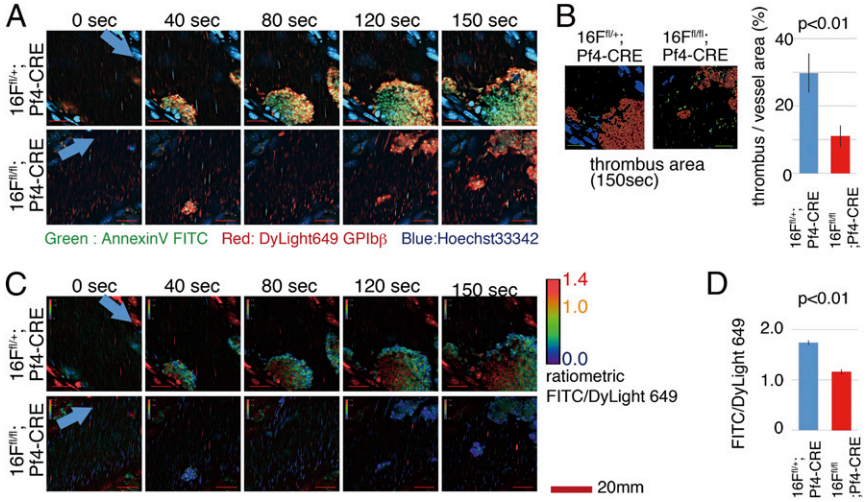

Fig. 5. Analysis of PtdSer exposure on platelets aggregated at a thrombus in a laser/ROS injury model. *TMEM16F*$^{fl/+}$;*Pf4-CRE* and *TMEM16F*$^{fl/fl}$;*Pf4-CRE* mice were injected with DyLight 649-anti-GP1bβmAb, FITC-Annexin V, Hoechst 33342, and hematoporphyrin. After anesthesia, the testicular vein was exposed and visualized by using a high-speed resonance scanning confocal microscope with highly sensitive GaAs detectors. Platelet aggregations were induced by photochemically induced ROS from hematoporphyrin within vessel lumens by laser irradiations. (*A*) Representative snap-shot raw images of developed thrombus. Note that the early responses of platelet aggressions were comparable in *TMEM16F*-deficient mice and control mice (40 s). However, the developed thrombus in *TMEM16F*-deficient mice was fragile, frequently collapsed by blood flow (80 s), and smaller in later phase (150 s) compared with the WT mice. Arrows indicate blood flow direction. (Scale bars: 20 μm.) (*B*) Quantification of thrombus area at 150 s using automatic software analysis ($n = 20$ vessels from $n = 5$ animals). (*C* and *D*) Ratiometric views and quantification analysis. Ratios are displayed in pseudocolor. Note that the FITC/DyLight 649 ratio increased within thrombus area in the WT mice, which was attenuated in *TMEM16F*-deficient mice. The FITC/DyLight 649 ratios were determined in 100 regions from 20 vessels from five animals, and the average values were plotted (*D*). We used ratiometric analysis to minimize the photobleaching effect by laser irradiation. The original videos are supplied as Movies S1*A* and S1*B* and S2*A* and S2*B*.

However, developed thrombus became fragile in a later phase, and was frequently collapsed by blood flow. Reflecting this instability, the thrombus area of *TMEM16F*-deficient mice was smaller when examined at 150 s after laser irradiation. In addition, we directly evaluated PtdSer exposure by injecting FITC-labeled Annexin V. In the WT mice, FITC signal within the thrombus area was gradually increased, indicating PtdSer exposure after platelet aggregations in vivo. However, this FITC signal increase was attenuated in *TMEM16F*-deficient mice (Fig. 5 *C* and *D* and Movies S1*A* and S1*B* and S2*A* and S2*B*). These results indicated that TMEM16F was indispensable for PtdSer exposure on activated platelets in vivo.

Discussion

Here, we report on the generation of mice with a platelet-specific deletion in *TMEM16F* and the effect of this deletion on the various functions of activated platelets. We demonstrated that TMEM16F was required for activation-induced PtdSer exposure, thrombin production, and microparticle release, but not for activation-induced α- and dense-granule release or thrombin-induced clot retraction. It did not affect tail vein bleeding time. These phenotypes are very similar to the phenotypes associated with human patients with Scott syndrome (7) and dogs with a similar hereditary syndrome (15), but significantly differ from the phenotypes previously associated with *TMEM16F*-null mice (13).

By using a convenient method to distinguish between ruptured platelets and intact activated platelets, we found that 37 °C-activated mouse platelets were fragile and their plasma membranes ruptured easily, in comparison with human platelets, which remained intact under those conditions. Notably, Yang et al. (13) activated mouse platelet at 37 °C for 30 min and did not see clear TMEM16F dependency on PtdSer exposure. PtdSer exposure in activated mouse platelets is also mediated by cyclophilin D-dependent Ca^{2+}-induced openings of the mitochondrial permeability transition pore (MPTP) (17, 32). These changes in MPTP lead to cell death, and mouse platelets may undergo MPTP more easily than human platelets. As PtdSer exposed on the compromised platelet membranes could contribute to thrombin generation, this may also account for the different thrombin phenotypes of *TMEM16*-deficient platelets reported here and by Yang et al. (13).

Platelet activation leads to dramatic changes in platelet morphology and the release of α- and dense granules. These granules are present in the cytoplasm, and are released as multivesicular bodies with exosome-like properties (33). Exosomes are transported from the cytoplasm to the plasma membrane by the actions of both RabGTPase and SNARE, and are released after fusion with the plasma membrane (34). On the contrary, microparticles express platelet membrane receptors, expose PtdSer on their surfaces, and play an important role in hemostasis and thrombosis (35). Microparticles are generated from platelet plasma membranes by shedding (36) in response to intracellular Ca^{2+} (37). We found that, when microparticle release was assessed by using activation conditions in which PtdSer exposure was strictly dependent on TMEM16F (20 °C and low Ca^{2+} concentrations), it was severely reduced in the absence of TMEM16F, although the release of α- and dense granules remained intact. Sims et al. (28) previously reported that the platelets from a patient with Scott syndrome exhibit defective microvesicle release, whereas another report suggested the involvement of calpain in the release of microparticles (38). We found that, when mouse platelets were treated with A23187 in the presence of 1 mM Ca^{2+}, microparticles were released from platelets in a TMEM16F-dependent manner. However, when the platelets were treated with A23187 in the presence of higher concentrations of Ca^{2+} (3 mM), the microparticles were released in a TMEM16F-independent, but calpain-dependent, manner. These results suggest that, under physiological conditions, TMEM16F plays an important role in microparticle shedding.

TMEM16F dependency has been similarly observed during bone tissue mineralization (39), during which PtdSer-rich matrix vesicles containing concentrated phosphate and Ca^{2+} ions bud off from the plasma membranes (40). Our EM images revealed that the rod-like extensions that formed on the surface of the activated platelets were released in a TMEM16F-dependent manner, consistent with the possibility that microparticle release from the activated platelets is associated with morphological changes. Given that the PtdSer-exposing plasma membranes of mouse platelets appear to be fragile, microparticle release may be a secondary event that follows PtdSer exposure.

As described earlier, the deletion of *TMEM16F* in mouse platelets had little effect on clot retraction or tail bleeding times. The apparently normal bleeding time observed in mice containing a platelet-specific *TMEM16F* deletion differs from the results of Yang et al. (13). This difference may result from the role of TMEM16F-mediated PtdSer scrambling in endothelial or vascular cells. However, this is unlikely because a patient with Scott syndrome who carries a defective TMEM16F gene in all tissues has a normal bleeding time (14). Munnix et al. (41) reported that there are two populations in activated platelets. One population of platelets that controls the generation of thrombin and fibrin exposes PtdSer, but does not express the activated αIIbβ3 integrin. On the contrary, the other population of platelets that controls clot retraction expresses the activated αIIbβ3 integrin, but does not expose PtdSer (41). Our results, showing that *TMEM16F*-null platelets were associated with reduced thrombin generation but normal clot retraction times, are consistent with this finding.

Our in vivo analysis showing reduced exposure of PtdSer on *TMEM16F*-null platelets also showed that damaged white blood cells present in the *TMEM16F*$^{fl/fl}$;*Pf4-CRE* mice exposed PtdSer. Thus, the PtdSer exposed on these cells may contribute to the generation of thrombin and fibrin in vivo, which could explain the mild coagulation defect in these mice and in patients with Scott syndrome. Taken together, the similarity in the phenotypes of the *TMEM16F*$^{fl/fl}$;*Pf4-CRE* mice and those of patients with Scott syndrome suggests that these mice may provide an ideal animal model for this disease.

Materials and Methods

Cell lines, reagents, genotyping of mouse mutants, EM, real-time PCR, flow cytometry, Western blotting, and ATP assay are described in *SI Materials and Methods*.

Mice. C57BL/6J mice were from Japan SLC. *TMEM16F*$^{fl/fl}$ mice were as described previously (5). Mice carrying *TMEM16F*-null platelets were generated by crossing *TMEM16F*$^{flox/+}$ mice with *Pf4-CRE* mice (25). The mice were housed in a specific pathogen-free facility at Kyoto University, and all animal experiments were performed in accordance with protocols approved by the animal care and use committees of Kyoto University and Osaka University.

Preparation of Washed Platelets and PFP. Platelets were prepared as described previously (42). In brief, for human platelets, blood was drawn into a one-sixth volume of acid-citrate-dextrose (ACD) buffer (41.6 mM citric acid, 85.3 mM trisodium-citrate buffer, pH 5.0, and 136 mM D-glucose). For mouse platelets, blood was collected by cardiac puncture from 8–12-wk-old mice that had been euthanized by CO_2 asphyxiation, and one-sixth volume of ACD buffer was added. Platelet-rich plasma (PRP) was obtained by centrifugation at 150 × *g* for 15 min. To obtain washed platelets, an equal volume of modified Tyrode buffer (Tyrode-H, 10 mM Hepes·NaOH buffer, pH 7.4, 12 mM $NaHCO_3$, 138 mM NaCl, 5.5 mM glucose, 2.9 mM KCl, and 1 mM $MgCl_2$), supplemented with 0.3 μM prostaglandin E_1 (PGE_1) and 15% (vol/vol) ACD, was added to PRP and centrifuged at 1,000 × *g* for 5 min. The precipitated platelets were washed with Tyrode-H buffer containing 0.15 μM PGE_1 and 1 mM EDTA, suspended in Tyrode-H buffer, and used as washed platelets. To obtain PFP, the ACD-treated mouse blood was successively centrifuged at 22 °C twice at 1,000 × *g* for 5 min and once at 20,000 × *g* for 30 min. The supernatant was recovered as PFP.

Assay for Thrombin. The thrombin generation was assayed according to Wielders et al. (8). In brief, 1.2×10^7 washed platelets in 54 μL of Tyrode-H buffer were mixed with 6 μL of mouse PFP in a 96-well plate and incubated at 20 °C for 15 min. Tyrode-H buffer (60 μL) supplemented with 0.2 mM Z-Gly-Gly-Arg-7-Amino-4-methylcoumarin (Z-GGR-AMC), 16.6 pmoles human tissue factor, and 16 mM $CaCl_2$ was added to each well and incubated at 20 °C, and the resulting fluorescence was detected at an excitation wavelength of 390 nm and emission wavelength of 460 nm by using a microplate reader (Infinite M200; TECAN). For microparticles, 1.2×10^7 washed platelets in 200 μL of Tyrode-H buffer containing 0.05% BSA and 1 mM $CaCl_2$ were treated at 20 °C for 5 min with 1 μM A23187. After stopping the reaction with 600 μL of Tyrode-H buffer containing 0.05% BSA and 2.7 mM EDTA, the platelets were removed by centrifuging twice at 1,000 × *g* at 4 °C for 5 min. Microparticles were collected from the supernatants by centrifugation at 20,000 × *g* for 30 min, and the thrombin activity was assayed as described earlier.

Intravital Microscopy and Thrombus Formation. Imaging analysis of thrombus formation and PtdSer exposure was performed as described previously (31) with some modifications. In brief, a mixture of Hoechst 33342 (10 mg/kg; Invitrogen), DyLight 649-anti-GP1bβmAb (0.2 mg/kg), and FITC-Annexin V (20 μL per mouse; BioLegend) was administered into anesthetized mice. Hematoporphyrin (1.8 mg/kg) was administrated to produce ROS upon laser irradiation. The mice were secured to the heated piezo-drive heating stage (Nikon and Tokai Hit) of an inverted microscope (Eclipse Ti; Nikon). Veins on the testicular epidermis were monitored during laser excitation at 405, 488, and 640 nm (1.5 mW power at objective lens). XYT sequential images were obtained with a resonance confocal microscope (A1; Nikon) using a 100× oil-immersion objective lens (NA 1.15; Nikon). Data were analyzed and visualized using an automatic algorithm in NIS-Elements (Nikon) and custom-designed software (IMAGICA Imageworks). Snap-shot XY and ratiometric images are provided in the figures and videos. Also calculated by the software were the developed thrombus area and time-dependent changes of ratiometric signals. Quantifications were performed automatically by software without parameter adjustment by observers.

ACKNOWLEDGMENTS. We thank K. Okamoto-Furuta and H. Kohda for the EM analysis, Radek C. Scoda for *Pf4-CRE* transgenic mice, H. Sakaguchi for software analysis, and M. Fujii for secretarial assistance. This work was supported in part by Grants-in-Aid from the Japan Society for the Promotion of Science (to S. Nagata).

1. Leventis PA, Grinstein S (2010) The distribution and function of phosphatidylserine in cellular membranes. *Annu Rev Biophys* 39:407–427.
2. Balasubramanian K, Schroit AJ (2003) Aminophospholipid asymmetry: A matter of life and death. *Annu Rev Physiol* 65:701–734.
3. Segawa K, et al. (2014) Caspase-mediated cleavage of phospholipid flippase for apoptotic phosphatidylserine exposure. *Science* 344(6188):1164–1168.
4. Suzuki J, Denning DP, Imanishi E, Horvitz HR, Nagata S (2013) Xk-related protein 8 and CED-8 promote phosphatidylserine exposure in apoptotic cells. *Science* 341(6144): 403–406.
5. Suzuki J, et al. (2013) Calcium-dependent phospholipid scramblase activity of TMEM16 protein family members. *J Biol Chem* 288(19):13305–13316.
6. Suzuki J, Umeda M, Sims PJ, Nagata S (2010) Calcium-dependent phospholipid scrambling by TMEM16F. *Nature* 468(7325):834–838.
7. Weiss HJ, Vicic WJ, Lages BA, Rogers J (1979) Isolated deficiency of platelet procoagulant activity. *Am J Med* 67(2):206–213.
8. Wielders SJ, et al. (2009) Absence of platelet-dependent fibrin formation in a patient with Scott syndrome. *Thromb Haemost* 102(1):76–82.
9. Toti F, Satta N, Fressinaud E, Meyer D, Freyssinet JM (1996) Scott syndrome, characterized by impaired transmembrane migration of procoagulant phosphatidylserine and hemorrhagic complications, is an inherited disorder. *Blood* 87(4):1409–1415.
10. Bevers EM, et al. (1992) Defective Ca(2+)-induced microvesiculation and deficient expression of procoagulant activity in erythrocytes from a patient with a bleeding disorder: A study of the red blood cells of Scott syndrome. *Blood* 79(2):380–388.
11. Kojima H, et al. (1994) Production and characterization of transformed B-lymphocytes expressing the membrane defect of Scott syndrome. *J Clin Invest* 94(6):2237–2244.
12. Castoldi E, Collins PW, Williamson PL, Bevers EM (2011) Compound heterozygosity for 2 novel TMEM16F mutations in a patient with Scott syndrome. *Blood* 117(16): 4399–4400.
13. Yang H, et al. (2012) TMEM16F forms a Ca^{2+}-activated cation channel required for lipid scrambling in platelets during blood coagulation. *Cell* 151(1):111–122.
14. Weiss HJ, Lages B (1997) Family studies in Scott syndrome. *Blood* 90(1):475–476.
15. Brooks MB, Catalfamo JL, Brown HA, Ivanova P, Lovaglio J (2002) A hereditary bleeding disorder of dogs caused by a lack of platelet procoagulant activity. *Blood* 99(7):2434–2441.
16. Versteeg HH, Heemskerk JWM, Levi M, Reitsma PH (2013) New fundamentals in hemostasis. *Physiol Rev* 93(1):327–358.
17. de Witt SM, Verdoold R, Cosemans JMEM, Heemskerk JWM (2014) Insights into platelet-based control of coagulation. *Thromb Res* 133(suppl 2):S139–S148.
18. Bevers EM, et al. (1995) The complex of phosphatidylinositol 4,5-bisphosphate and calcium ions is not responsible for Ca2+-induced loss of phospholipid asymmetry in the human erythrocyte: A study in Scott syndrome, a disorder of calcium-induced phospholipid scrambling. *Blood* 86(5):1983–1991.
19. Jobe SM, et al. (2008) Critical role for the mitochondrial permeability transition pore and cyclophilin D in platelet activation and thrombosis. *Blood* 111(3):1257–1265.
20. Vermes I, Haanen C, Steffens-Nakken H, Reutelingsperger C (1995) A novel assay for apoptosis. Flow cytometric detection of phosphatidylserine expression on early apoptotic cells using fluorescein labelled Annexin V. *J Immunol Methods* 184(1):39–51.
21. Hanayama R, et al. (2002) Identification of a factor that links apoptotic cells to phagocytes. *Nature* 417(6885):182–187.
22. Wulf E, Deboben A, Bautz FA, Faulstich H, Wieland T (1979) Fluorescent phallotoxin, a tool for the visualization of cellular actin. *Proc Natl Acad Sci USA* 76(9):4498–4502.
23. Watanabe-Fukunaga R, Brannan CI, Copeland NG, Jenkins NA, Nagata S (1992) Lymphoproliferation disorder in mice explained by defects in Fas antigen that mediates apoptosis. *Nature* 356(6367):314–317.
24. Shiraishi T, et al. (2004) Increased cytotoxicity of soluble Fas ligand by fusing isoleucine zipper motif. *Biochem Biophys Res Commun* 322(1):197–202.
25. Tiedt R, Schomber T, Hao-Shen H, Skoda RC (2007) Pf4-Cre transgenic mice allow the generation of lineage-restricted gene knockouts for studying megakaryocyte and platelet function in vivo. *Blood* 109(4):1503–1506.
26. Munnix ICA, Cosemans JMEM, Auger JM, Heemskerk JWM (2009) Platelet response heterogeneity in thrombus formation. *Thromb Haemost* 102(6):1149–1156.
27. Jonnalagadda D, Izu LT, Whiteheart SW (2012) Platelet secretion is kinetically heterogeneous in an agonist-responsive manner. *Blood* 120(26):5209–5216.
28. Sims PJ, Wiedmer T, Esmon CT, Weiss HJ, Shattil SJ (1989) Assembly of the platelet prothrombinase complex is linked to vesiculation of the platelet plasma membrane. Studies in Scott syndrome: An isolated defect in platelet procoagulant activity. *J Biol Chem* 264(29):17049–17057.
29. McCarty OJT, et al. (2005) Rac1 is essential for platelet lamellipodia formation and aggregate stability under flow. *J Biol Chem* 280(47):39474–39484.
30. Sinauridze EI, et al. (2007) Platelet microparticle membranes have 50- to 100-fold higher specific procoagulant activity than activated platelets. *Thromb Haemost* 97(3): 425–434.
31. Nishimura S, et al. (2012) In vivo imaging visualizes discoid platelet aggregations without endothelium disruption and implicates contribution of inflammatory cytokine and integrin signaling. *Blood* 119(8):e45–e56.
32. Mattheij NJA, et al. (2013) Dual mechanism of integrin αIIbβ3 closure in procoagulant platelets. *J Biol Chem* 288(19):13325–13336.
33. Heijnen HF, Schiel AE, Fijnheer R, Geuze HJ, Sixma JJ (1999) Activated platelets release two types of membrane vesicles: Microvesicles by surface shedding and exosomes derived from exocytosis of multivesicular bodies and alpha-granules. *Blood* 94(11): 3791–3799.
34. Kowal J, Tkach M, Théry C (2014) Biogenesis and secretion of exosomes. *Curr Opin Cell Biol* 29:116–125.
35. Burnouf T, Goubran HA, Chou M-L, Devos D, Radosevic M (2014) Platelet microparticles: detection and assessment of their paradoxical functional roles in disease and regenerative medicine. *Blood Rev* 28(4):155–166.
36. Théry C, Ostrowski M, Segura E (2009) Membrane vesicles as conveyors of immune responses. *Nat Rev Immunol* 9(8):581–593.
37. Dachary-Prigent J, Pasquet JM, Freyssinet JM, Nurden AT (1995) Calcium involvement in aminophospholipid exposure and microparticle formation during platelet activation: A study using Ca2+-ATPase inhibitors. *Biochemistry* 34(36):11625–11634.
38. Pasquet JM, Dachary-Prigent J, Nurden AT (1996) Calcium influx is a determining factor of calpain activation and microparticle formation in platelets. *Eur J Biochem* 239(3):647–654.
39. Ehlen HW, et al. (2013) Inactivation of anoctamin-6/Tmem16f, a regulator of phosphatidylserine scrambling in osteoblasts, leads to decreased mineral deposition in skeletal tissues. *J Bone Miner Res* 28(2):246–259.
40. Damek-Poprawa M, et al. (2006) Chondrocytes utilize a cholesterol-dependent lipid translocator to externalize phosphatidylserine. *Biochemistry* 45(10):3325–3336.
41. Munnix ICA, et al. (2007) Segregation of platelet aggregatory and procoagulant microdomains in thrombus formation: Regulation by transient integrin activation. *Arterioscler Thromb Vasc Biol* 27(11):2484–2490.
42. Takizawa H, et al. (2010) Lnk regulates integrin alphaIIbbeta3 outside-in signaling in mouse platelets, leading to stabilization of thrombus development in vivo. *J Clin Invest* 120(1):179–190.
43. Chida J, Kido H (2014) Extraction and quantification of adenosine triphosphate in mammalian tissues and cells. *Methods Mol Biol* 1098:21–32.